

## Article

# Mobile DOAS Observations of Tropospheric NO<sub>2</sub> Using an UltraLight Trike and Flux Calculation

Daniel-Eduard Constantin <sup>1,\*</sup>, Alexis Merlaud <sup>2</sup>, Mirela Voiculescu <sup>1</sup>, Carmelia Dragomir <sup>1</sup>, Lucian Georgescu <sup>1</sup>, Francois Hendrick <sup>2</sup>, Gaia Pinardi <sup>2</sup> and Michel Van Roozendaal <sup>2</sup>

<sup>1</sup> European Center of Excellence for the Environment, Faculty of Sciences and Environment, “Dunarea de Jos” University of Galati, Str. Domneasca 111, Galati 800008, Romania; mirela.voiculescu@ugal.ro (M.V.); carmelia.dragomir@ugal.ro (C.D.); lucian.georgescu@ugal.ro (L.G.)

<sup>2</sup> Royal Belgian Institute for Space Aeronomy, Ringlaan-3-Avenue Circulaire, B-1180 Brussels, Belgium; alexis.merlaud@aeronomie.be (A.M.); francois.hendrick@aeronomie.be (F.H.); gaia.pinardi@aeronomie.be (G.P.); michel.vanroozendaal@aeronomie.be (M.V.R.)

\* Correspondence: daniel.constantin@ugal.ro

Academic Editors: Pius Lee, Rick Saylor and Jeff McQueen

Received: 24 February 2017; Accepted: 19 April 2017; Published: 22 April 2017

**Abstract:** In this study, we report on airborne Differential Optical Absorption Spectroscopy (DOAS) observations of tropospheric NO<sub>2</sub> using an Ultralight Trike (ULT) and associated flux calculations. The instrument onboard the ULT was developed for measuring the tropospheric NO<sub>2</sub> Vertical Column Density (VCD) and it was operated for several days between 2011 and 2014, in the South-East of Romania. Collocated measurements were performed using a car-DOAS instrument. Most of the airborne and mobile ground-based measurements were performed close to an industrial platform located nearby Galati city (45.43° N, 28.03° E). We found a correlation of  $R = 0.71$  between tropospheric NO<sub>2</sub> VCDs deduced from airborne DOAS observations and mobile ground-based DOAS observations. We also present a comparison between stratospheric NO<sub>2</sub> Slant Column Density (SCD) derived from the Dutch OMI NO<sub>2</sub> (DOMINO) satellite data product and stratospheric SCDs obtained from ground and airborne measurements. The airborne DOAS observations performed on 13 August 2014 were used to quantify the NO<sub>2</sub> flux originating from an industrial platform located nearby Galati city. Measurements during a flight above the industrial plume showed a maximum tropospheric NO<sub>2</sub> VCD of  $(1.41 \pm 0.27) \times 10^{16}$  molecules/cm<sup>2</sup> and an associated NO<sub>2</sub> flux of  $(3.45 \pm 0.89) \times 10^{-3}$  kg/s.

**Keywords:** mobile DOAS; airborne observations; nitrogen dioxide; emission flux

## 1. Introduction

Nitrogen dioxide (NO<sub>2</sub>) is a chemical gaseous compound with an important role in the Earth's atmosphere. NO<sub>2</sub> is a key trace element in the chemistry of ozone, since it is involved in the catalytic destruction of ozone in the stratosphere [1], while in the troposphere its photolysis leads directly to the formation of ozone (O<sub>3</sub>) in the presence of VOCs (volatile organic compounds). NO<sub>2</sub> is released in the atmosphere from natural sources (soil, lightning, solar cosmic rays) and anthropogenic emissions (fossil fuels and biomass burning, industrial activities). Long-term exposure to NO<sub>2</sub> may affect the respiratory system and lead to coronary diseases. NO<sub>2</sub> can lead to acidification of the aquatic ecosystem following the oxidation to HNO<sub>3</sub>.

The Differential Optical Absorption Spectroscopy (DOAS) technique [2] has been used for NO<sub>2</sub> atmospheric measurements since the early 1970s [3,4]. Nowadays, besides ground-based zenith sky measurements, DOAS techniques have developed into Multi-Axis Differential Optical Absorption Spectroscopy (MAX-DOAS) observations [5]. The mobile DOAS technique was recently used on

several platforms such as: cars [6,7], airplanes [8–10], Unmanned Aerial Vehicles (UAVs) [11] or satellites [12–16].

Airborne observations have a number of important advantages for atmospheric research such as: the flexibility during the flights and the possibility to access remote areas such as oceans, deserts, rural or areas without roads.

The ULMs (Ultralight Motorized) are airborne platforms with an important scientific potential for atmospheric research. So far, ULMs have been used to study the ultraviolet actinic radiation flux [17], formaldehyde distribution [18], aerosol profiles [19],  $\text{SO}_2$ ,  $\text{NO}_2$  and ozone distribution [20–23].

This work highlights the capability of a low-cost system (ULT-DOAS) used for measurements of tropospheric  $\text{NO}_2$  VCD and associated flux calculations. This study presents airborne DOAS observations of tropospheric  $\text{NO}_2$  using an Ultralight Trike (ULT) and associated flux calculations. The work presented here was motivated by the need to further assess the intrapixel variability of  $\text{NO}_2$  detected by UV-VIS DOAS instruments onboard satellites. This work comes in the context of a validation programme of the future Atmospheric Sentinels, starting with the Sentinel-5 Precursor to be launched in summer 2017. A similar system based on DOAS onboard the ULM was used during the Airborne Romanian Measurements of Aerosols and Trace gases (AROMAT) campaign, held in Romania in August 2015 [24]. The AROMAT campaign was conducted under the aegis of the European Space Agency (ESA) in the framework of a series of ESA field campaigns.

## 2. Methodology

### 2.1. Experimental and Instrumental Descriptions

The mobile DOAS observations were performed onboard of an Ultralight Trike (ULT), in the South-East of Romania (Figure 1) during several days between 2011 and 2014. All measurements were performed under clear-sky conditions (see Table 1). The Mobile DOAS system used for measurements will be described in the following as the ULT-DOAS system. The measurements took place in an area around Galati (located at  $45.43^\circ \text{ N}$ ,  $28.03^\circ \text{ E}$ ), Braila ( $45.26^\circ \text{ N}$ ,  $27.95^\circ \text{ E}$ ), and close to the industrial areas of Slobozia ( $44.56^\circ \text{ N}$ ,  $27.35^\circ \text{ E}$ ). Note that an operational steel mill factory is located in the vicinity of Galati, while Slobozia was chosen due to the presence of a fertilizer factory. Due to security concerns, direct flights above the cities or industrial platforms were not performed. Most of the airborne DOAS observations were performed in nadir geometry. Details about the ULT-DOAS measurements are presented in Table 1.

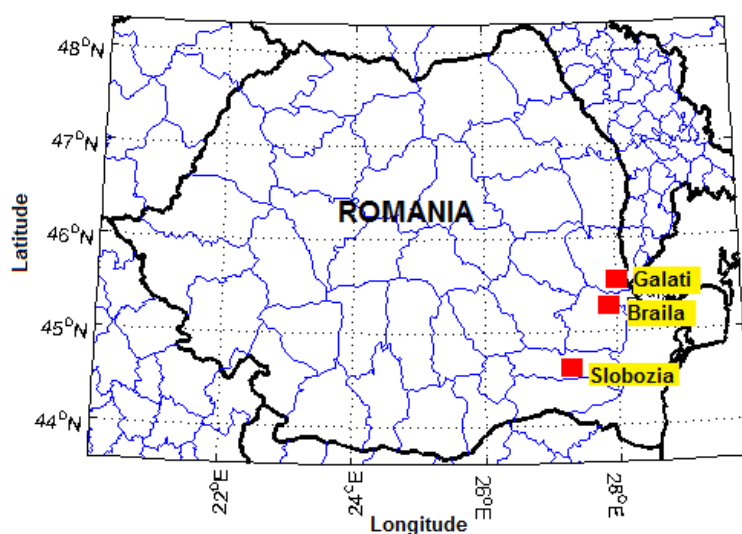


**Figure 1.** The main locations where airborne and/or ground-based mobile Differential Optical Absorption Spectroscopy (DOAS) observations were performed.

**Table 1.** Coordinates and temporal coverage of the mobile DOAS measurements.

Day	Time Interval UTC *	Route of ULT-DOAS ** Measurements	NO <sub>2</sub> Source Target
1 September 2011	8.31–9.45	Galati–Braila	Braila urban area
25 August 2012	7.53–8.89	Galati–Braila	Braila urban area
21 July 2014	9.51–10.96	Galati–Slobozia	Slobozia industrial area
13 August 2014	7.32–8.19	Galati	Galati industrial area

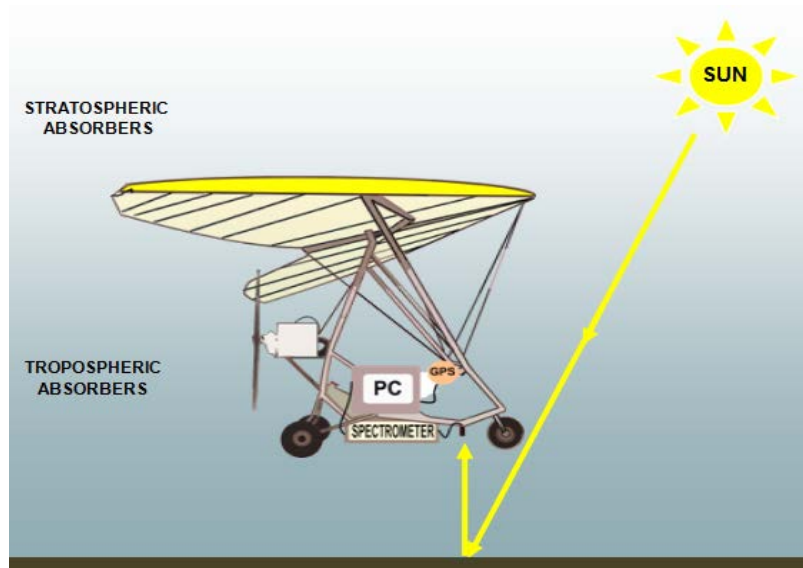
\* Coordinated Universal Time. \*\* ULT-DOAS = Ultralight Trike-Differential Optical Absorption Spectroscopy.

Airborne-DOAS measurements were accompanied by car-DOAS measurements and static twilight observations on 21 July 2014. Static twilight DOAS measurements, used for determination of the NO<sub>2</sub> content from the reference spectra, were performed in a rural area close to Galati city. The car-DOAS measurements were performed right before or after the experimental flights.

The aircraft used for all the flight experiments presented in this paper is a double-seated, open-cockpit ultralight aircraft, trike type (model Fanagoria 21, produced by Plovdiv Air Bulgaria). The flexible wing (Atlant-21, produced by Plovdiv Air Bulgaria) has an area of 16 m<sup>2</sup>. The ULT is powered by a Subaru EA81 engine with 75 HP. The cruise speed is 75 km/h and the maximum speed is 100 km/h relative to the ground. The aircraft has a maximum total weight at take-off of 450 kg.

The ULT-DOAS instrument consists of a compact Czerny–Turner spectrometer (AvaSpec-ULS2048XL-USB2, of 175 × 110 × 44 mm dimensions and 855 g weight) placed in the Ultralight Trike. Figure 2 presents the instrumental DOAS set-up. The spectral range of the spectrometer is 280–550 nm with 0.7 nm resolution (FWHM—Full Width at Half Maximum) with a focal length of 75 mm. The entrance slit is 50 µm and the grating is 1200 L/mm, blazed at 250 nm. The spectrometer is connected to the telescope through a 400 µm chrome-plated brass optical fiber. The telescope achieves a 2.3° field-of-view with fused silica collimating lenses. Each spectrum is recorded by a laptop and georeferenced by a GPS receiver. The spectrometer and the GPS receiver are powered by the laptop USB ports. The entire set-up is powered by 12 V of the ULT through an inverter. Each measurement is a 10-second average of 10 scans accumulations at an integration time between 50 and 150 ms.

This work is mostly based on nadir-DOAS observations but we also present zenith-sky observations onboard ULT for stratospheric NO<sub>2</sub> measurements. The same DOAS system was used in the case of the zenith sky car-DOAS observations.

**Figure 2.** Schematic of the ULT-DOAS measurement principle.

## 2.2. Determination of the NO<sub>2</sub> Tropospheric Vertical Column and Flux Calculation

### 2.2.1. Retrieval of NO<sub>2</sub> Slant Column

The analysis of the measured spectra was performed using the QDOAS software [25]. For the NO<sub>2</sub> fit, the spectral window of 425–490 nm was used. The NO<sub>2</sub> spectral analysis included five absorption cross sections: the NO<sub>2</sub> cross sections at 298 K and 220 K [26], the O<sub>3</sub> cross section at 223 K [27], the O<sub>4</sub> cross section [28] and a Ring spectrum [29]. A fifth-degree polynomial to account for scattering processes and broad-band absorption in the atmosphere was used in the DOAS analysis. The direct result of the spectral analysis is a differential slant column density (DSCD), which is the integrated trace gas concentration along the light path through the atmosphere. The DSCD is the difference between the slant column densities in the measured spectra (SCD<sub>meas</sub>) and the Fraunhofer reference spectrum (SCD<sub>ref</sub>). The NO<sub>2</sub> amount in the Fraunhofer reference spectrum is unknown and its retrieval is important for the determination of the SCD<sub>meas</sub> (Equation (1)).

$$\text{SCD}_{\text{meas}} = \text{DSCD} + \text{SCD}_{\text{ref}} \quad (1)$$

Figure 3 presents a typical DOAS fit using a spectrum recorded during the experiment close to the Galati steel factory, on 13 August 2014.

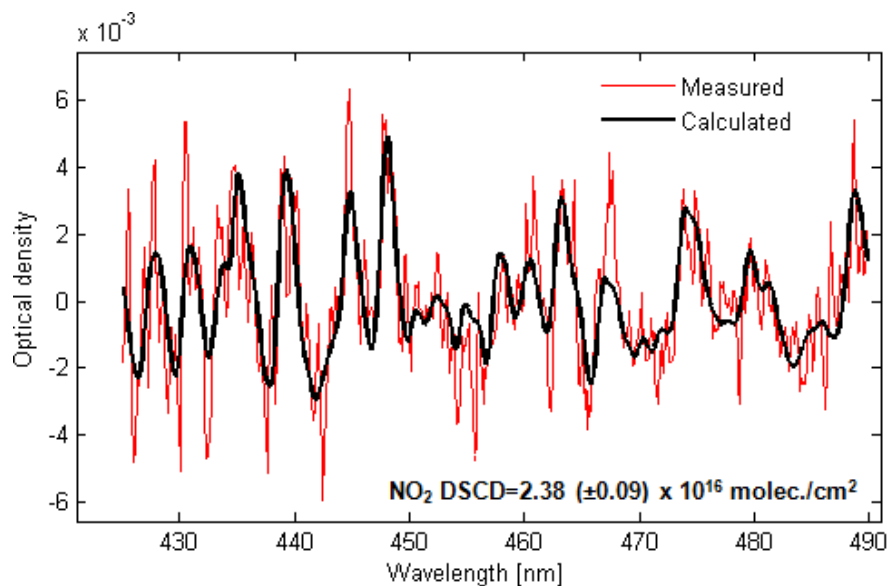


**Figure 3.** Example of a DOAS fit realized with the QDOAS software; the analyzed spectrum was recorded close to Galati, on 13 August 2014. Black line corresponds to molecular cross sections scaled to the detected absorptions in the measured spectrum (red line).

The Slant Column Density (SCD) is converted to a Vertical Column Density (VCD) by means of an Air Mass Factor (AMF), which is defined as the ratio between SCD and VCD (Equation (2))

$$\text{AMF} = \frac{\text{SCD}}{\text{VCD}} = \frac{\tau_{\text{SCD}}}{\tau_{\text{VCD}}} \quad (2)$$

where  $\tau_{\text{SCD}}$  and  $\tau_{\text{VCD}}$  are the optical thickness for the slant column (SCD) and vertical column (VCD), respectively.

Since the measured spectra contain information about both stratospheric and tropospheric NO<sub>2</sub> content, the SCD<sub>meas</sub> can be written as:

$$\text{SCD}_{\text{meas}} = \text{AMF}_{\text{tropo}} \cdot \text{VCD}_{\text{tropo}} + \text{AMF}_{\text{strato}} \cdot \text{VCD}_{\text{strato}} - \text{SCD}_{\text{ref}} \quad (3)$$

The above equations can be further simplified assuming that  $SCD_{ref}$  is dominated by stratospheric  $NO_2$ . Using this assumption, the stratospheric contributions can be canceled by the  $NO_2$  amount in the reference spectrum (Equation (4)) [8].

$$VCD_{tropo} = DSCD / AMF_{tropo} \quad (4)$$

The assumption presented above is valid if the reference spectrum (needed for the spectral evaluation) is recorded at noon, in an area with a very low  $NO_2$  content and if  $SCD_{strato}$  does not vary in time. The Fraunhofer reference spectrum could also be a zenith-sky spectrum recorded at high altitude over the boundary layer [30]. However, in this work the tropospheric  $NO_2$  VCD is based on calculations using Equation (3).

### 2.2.2. Deduction of the $SCD_{ref}$ and $VCD_{strato}$

To avoid systematic errors due to the use of multiple reference spectra, only one spectrum will be used for the spectral analysis of all DOAS observations presented in this paper.

The  $NO_2$  amount in the reference spectrum was calculated using a photo-chemically modified Langley plot [6,31]. The  $SCD_{ref}$  corresponds to a zenith spectrum recorded at noon, in a clean rural area close to Galati city. The spectrum was recorded on 13 August 2014 (9.70 UTC and solar zenith angle (SZA) = 31.55°).

The photo-chemically modified Langley plot was applied for the twilight sunrise observations performed on 21 July 2014. By applying the Langley plot method, we calculated the  $SCD_{ref}$  as  $4.1 \times 10^{15}$  molecules/cm<sup>2</sup> of  $NO_2$ .

The stratospheric contribution used for the retrieval of the  $VCD_{tropo}$  is derived from the assimilated vertical stratospheric columns simulated by Dutch OMI  $NO_2$  (DOMINO). Table 2 shows the satellite overpass data sets that were used for the retrieval algorithm presented in this work.

**Table 2.** OMI satellite overpasses data sets.

Day	Orbit Nr.	Overpass Time UTC	Stratospheric VCD [ $\times 10^{15}$ molecules/cm <sup>2</sup> ]
1 September 2011	37,923	11:04:28	3.76
25 August 2012	43,151	11:11:07	3.75
21 July 2014	53,272	11:17:36	4.14
13 August 2014	53,607	11:23:47	3.74

VCD = Vertical Column Density.

Figure 4A presents the SCD determined at twilight sunrise on 21 July 2014 compared with the  $SCD_{strato}$  derived from the DOMINO Level 2 product [32] scaled with a chemically modified AMF calculated by PSCBOX [33,34]. More details about the retrieval of the  $SCD_{strato}$  using twilight observations and model simulations are presented in [6]. A good agreement between the two types of  $SCD_{strato}$  determinations is obtained, which gives confidence in the stratospheric SCD measured by our static DOAS observations.

Figure 4B shows the  $SCD_{strato}$  derived from DOMINO compared with the SCDs determined by car-DOAS zenith-sky observations and ULT-DOAS measurements performed in the zenith geometry, for the same day of 21 July 2014. From this plot, one can see that the car-DOAS measurements are dominated by tropospheric  $NO_2$  while the zenith-sky ULT-DOAS observation presents a low amount of  $NO_2$  close to the stratospheric  $NO_2$  SCD derived from OMI. This is due to the fact that zenith-sky ULT-DOAS observations are performed above the  $NO_2$  plume or above the planetary boundary layer.

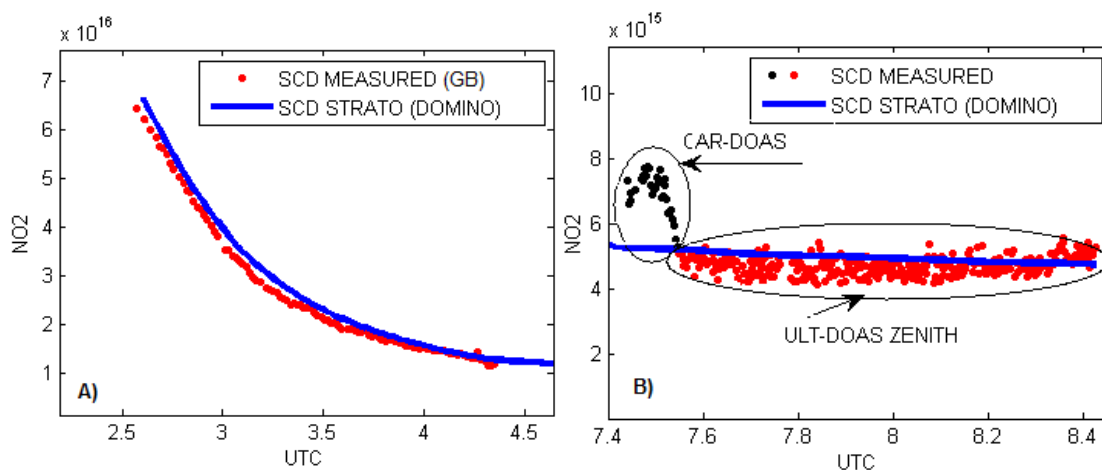


**Figure 4.** Comparisons between measured SCD using various methods of determination and stratospheric SCD derived from OMI (21 July 2014); **(A)** Comparison between SCD determined from ground-based (GB) observations and stratospheric SCD derived from DOMINO; **(B)** Comparison between SCD determined from CAR-DOAS (black dots) and ULT-DOAS (red dots) and stratospheric SCD derived from DOMINO.

### 2.2.3. Radiative Transfer Calculation

In order to determine the VCD, the SCD retrieved with the DOAS method has to be converted using an appropriate AMF. The geometric approximation for the airborne DOAS observations assumes a simple reflection of the sunlight on the earth's surface. In this case (neglecting the earth's sphericity) the nadir AMF can be described as a function of the solar zenith angle (SZA) as:

$$\text{AMF}_{\text{geo}} = 1 + 1/\cos(\text{SZA}) \quad (5)$$

Since the ULT-DOAS measurements were performed in the open atmosphere using scattered sunlight radiation, the radiative transfer during the observations needs to be modeled to interpret the retrieved data. In this work, the AMF was calculated using the radiative transfer model (RTM) UVspec/DISORT [35], which is a fully spherical model. This RTM has been validated using six other different codes [34].

The general assumptions made for the radiative transfer calculation using the RTM UVspec/DISORT are introduced in Table 3.

**Table 3.** Input parameters used for the radiative transfer model (RTM) calculations.

Trace Gas	Nitrogen Dioxide		
wavelength	440 nm		
flight altitude	1000 m		1500 m
albedo		0.1	
visibility	1 km	5 km	20 km
line of sight		0°	

Results of AMF simulations for the nadir flight performed on 13 August 2014, using the input parameters presented in Table 3, are displayed in Figure 5. The geometric AMF for the nadir view is also shown. The visibility parameter accounts for the effect of aerosols.



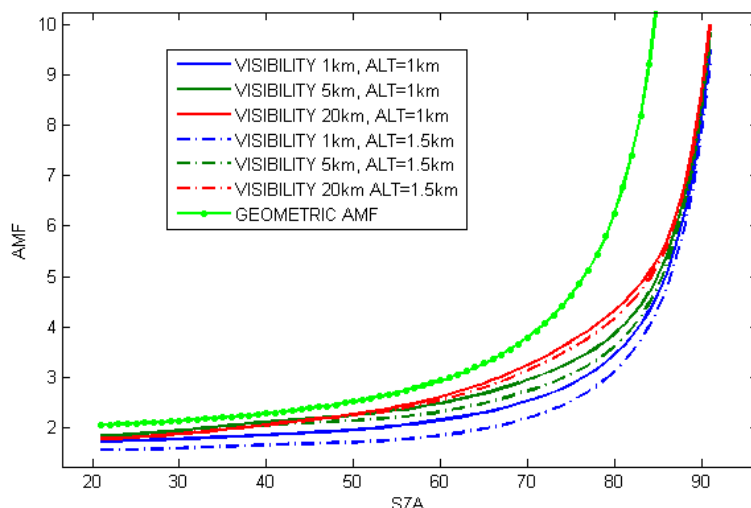


**Figure 5.** AMF simulations obtained from RTM calculations using UVspec/DISORT for various input parameters, for 13 August 2014. AMF = Air Mass Factor.

### 3. Results and Discussions

The airborne DOAS observations were designed to determine the distribution of tropospheric  $\text{NO}_2$  from the South-East of Romania from urban, industrial and rural areas and associated flux.

The first flights were performed on 1 September 2011 and 25 August 2012, and aimed at measuring the  $\text{NO}_2$  around the industrial area of Galati city and from Braila city. The flight performed on 21 July 2014 aimed to measure the  $\text{NO}_2$  emitted by a fertilizer factory located nearby Slobozia city; unfortunately, during the DOAS flight the fertilizer factory was not operational. Figure 6 presents the horizontal distribution of the tropospheric  $\text{NO}_2$  determined in nadir geometry for 1 September 2011, while Figure 7 depicts the results during a similar flight, but on 25 August 2012. During this experiment, the plume from the industrial platform was not fully crossed by the optical instrument onboard the ULT. The wind was northerly resulting in local increases of the  $\text{NO}_2$  amount detected by the spectrometer. The maximum tropospheric  $\text{NO}_2$  VCD detected during this experiment was  $(1.1 \pm 0.24) \times 10^{16}$  molecules/ $\text{cm}^2$  while the minimum tropospheric  $\text{NO}_2$  VCD was  $(2.1 \pm 0.81) \times 10^{15}$  molecules/ $\text{cm}^2$ .

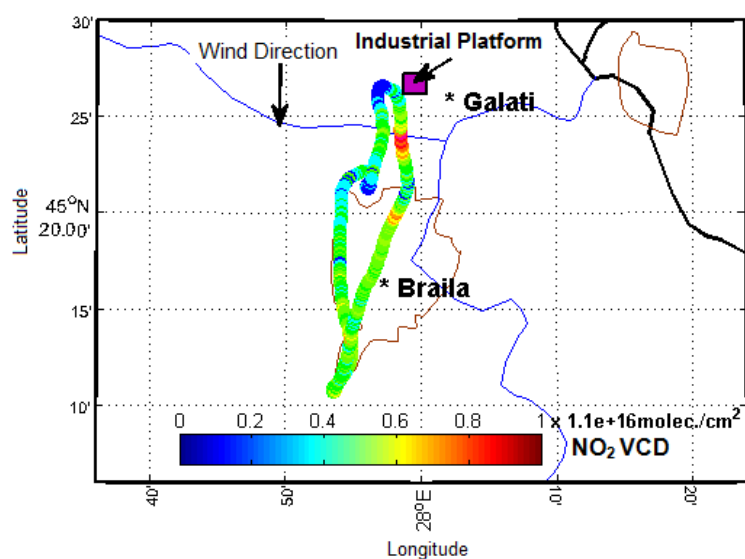


**Figure 6.** Map of tropospheric  $\text{NO}_2$  VCD determined on 1 September 2011 using ULT-DOAS observations.

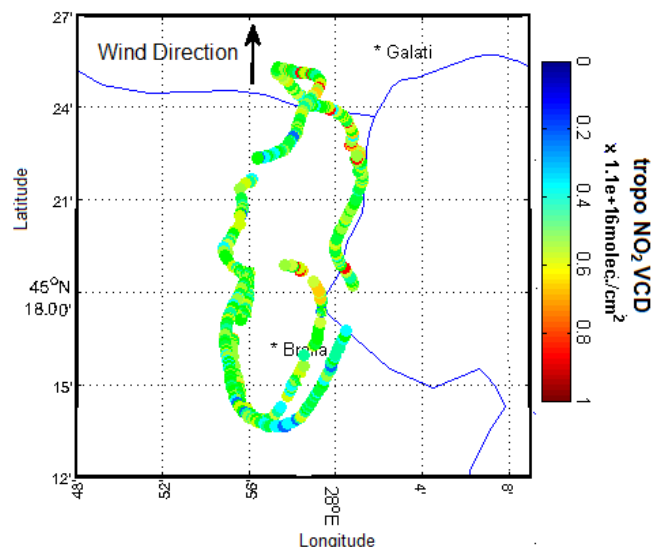


**Figure 7.** Map of tropospheric NO<sub>2</sub>VCD determined on 25 August 2012 using ULT-DOAS observations.

The trajectory of the flight on 13 August 2014 gave us the opportunity of calculating the NO<sub>2</sub> flux emissions around the industrial area of Galati city. This was not possible for the other flights because encircling the NO<sub>2</sub> source was not authorized.

On 1 September 2011, the NO<sub>2</sub> amount was low relative to the other day. The flight comprised almost two complete circles around Braila; however, the NO<sub>2</sub> displayed no clear variation. The horizontal distribution of NO<sub>2</sub> was quite homogenous over Braila city on this day.

A double experiment was performed on 13 August 2014, using both a ULT-DOAS and a car-based DOAS system. The mobile ground-based DOAS observations were performed using the same equipment during 9.75–10 UTC, while the ULT-DOAS observations were performed during 7.30–8.15 UTC.

Figure 8 shows the tropospheric NO<sub>2</sub> VCD derived along the trajectory of the ULT-DOAS measurements. The right plot shows a photograph of the plume crossed by the ULT flights. During the same day, approximately 1 h after the acquisition of the ULT-DOAS measurements, a zenith-sky car-DOAS system was used to sample the NO<sub>2</sub> plume at the same location as the ULT-DOAS observations. We assume that the quantity of the NO<sub>2</sub> emitted by the steel factory was almost constant during the airborne and car-DOAS system.

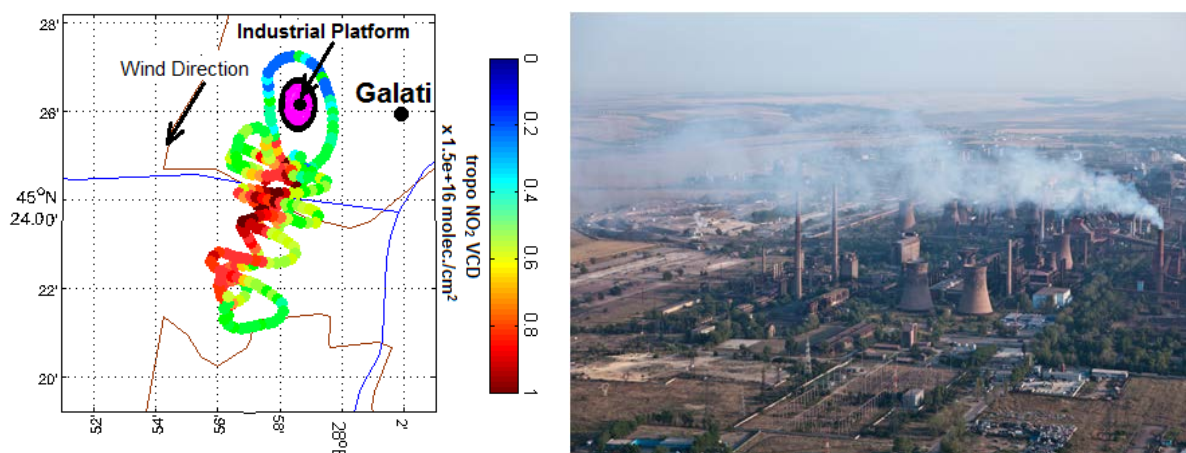
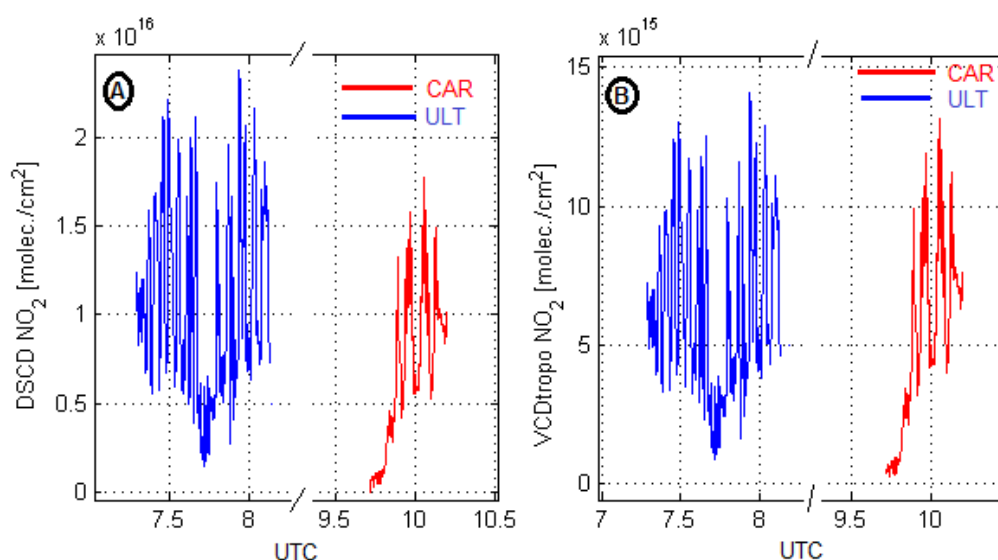


**Figure 8.** The tropospheric NO<sub>2</sub> VCD along the flight trajectory using the ULT-DOAS system on 13 August 2014 (left); Photography of the NO<sub>2</sub> plume determined on the same day (right).

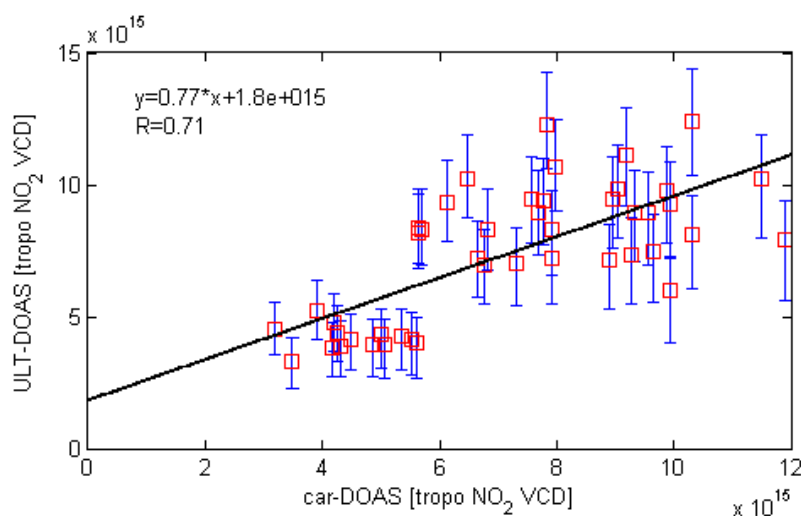


Figure 9 presents the  $\text{NO}_2$  VCD derived from the nadir airborne DOAS observations performed over the industrial area of Galati city compared with zenith-sky ground-based mobile DOAS measurements performed over the same area in the same day (13 August 2014). In these figures, we show the original SCDs (A) and the retrieved tropospheric  $\text{NO}_2$  VCD (B). Figure 9A shows that the DSCDs determined from the ULT-DOAS system are ~30% higher than the DSCDs determined using car-DOAS observations. This difference is attributed to the different observation geometries. After appropriate AMF calculation (see Section 2.2.2), both observations show close results.

The ULT flight above the industrial plume led to the detection of a maximum tropospheric  $\text{NO}_2$  VCD of  $(1.41 \pm 0.27) \times 10^{16}$  molecules/ $\text{cm}^2$  while the car-DOAS observation shows a maximum tropospheric  $\text{NO}_2$  VCD of  $(1.36 \pm 0.21) \times 10^{16}$  molecules/ $\text{cm}^2$ . Figure 10 displays the correlation between the tropospheric  $\text{NO}_2$  VCD retrieved by the ULT-DOAS and the car-DOAS instrument, where closest spatially coincident data were selected. A Pearson correlation coefficient  $R = 0.71$  was obtained between ground mobile DOAS observations and airborne DOAS measurements.



**Figure 9.** Comparisons between ULT-DOAS and car-DOAS observations performed on 13 August 2014. (A) The results of the preliminary DOAS analysis (DSCDs) and (B) after determination of the vertical columns (VCDs).



**Figure 10.** Correlation between tropospheric VCDs measured by the ULT-DOAS and the car-DOAS instrument on 13 August 2014.

### NO<sub>2</sub> Flux Calculation

The NO<sub>2</sub> flux above the industrial platform located nearby Galati city was calculated by performing upwind and downwind measurements around the point source using ULT-DOAS observations on 13 August 2014. The calculation of the emission flux is based on the following parameters: the NO<sub>2</sub> VCD determined from the transect over the plume, the wind speed and the wind factor correction, taking into account the angle between the flight direction and wind direction (Equation (6)), [20,36,37]:

$$\text{Flux}_{\text{NO}_2} = \sum_i \text{VCD}_{\text{NO}_2}(s_i) \cdot v \cdot \sin(\alpha_i) \cdot \Delta s_i \quad (6)$$

where  $\text{VCD}_{\text{NO}_2}$  is the NO<sub>2</sub> tropospheric vertical column,  $v$  is the wind speed,  $\alpha$  the angle between wind direction and driving route,  $i$  is the observations index, and  $\Delta s_i$  is the distance between two successive spectra.

The wind data used for the NO<sub>2</sub> flux calculation rely on measurements of the automatic weather station (Davis Vantage Pro2) located in the campus university of Galati city (45.44° N, 28.05° E), while vertical wind profiles come from the Hybrid Single Particle Lagrangian Integrated Trajectory Model (HYSPLIT) [38] model using archived dataset GDAS 0.5° × 0.5°. The weather station is located at 30 m height and acquires data every 30 min. Since no atmospheric sounding was possible during the experiments, the wind measured on the ground was scaled to the output of HYSPLIT model simulation at 1000 m altitude. During the period of the ULT-DOAS measurements, the mean NO<sub>2</sub> emission flux was determined to be  $(3.45 \pm 0.89) \times 10^{-3}$  kg/s. A local environmental report indicates ~600 tons/year NO<sub>x</sub> emissions emitted by the steel factory [39]. Using a Leighton ratio ( $L = [\text{NO}]/[\text{NO}_2]$ ) of 0.3, we calculated that the steel factory has emitted a mean of  $\sim 10 \times 10^{-3}$  kg/s of NO<sub>2</sub>. The difference between the two types of estimation may be attributed to the fact that the NO<sub>x</sub> emissions from the steel factory are dependent on the quantity of the steel produced, which can vary from one day to another. Also, the derived NO<sub>2</sub> fluxes must be dealt with some care because of the probably incomplete NO to NO<sub>2</sub> conversion [40].

## 4. Conclusions

Ultralight-trike DOAS observations were performed in the South-East of Romania during four days between 2011 and 2014. The first two flights were focused over Braila city, the third aimed at measurements of the NO<sub>2</sub> plume emitted by a fertilizer factory near Slobozia city. Unfortunately, during the DOAS flight the fertilizer factory was not operational. The last flight, performed on 13 August 2014, was focused over the industrial area of Galati city. Nadir observations were performed around the industrial platform of Galati city aiming at measuring the tropospheric NO<sub>2</sub> VCD around the source and at evaluating the associated NO<sub>2</sub> flux. To retrieve the tropospheric NO<sub>2</sub> VCD from ULT-DOAS observations, complementary ground- and space-based measurements were used.

We showed that the tropospheric NO<sub>2</sub> VCD deduced from the ULT-DOAS observations are consistent with measurements performed from the ground using a zenith-sky car-DOAS system. Although two hours separated the two experiments, a correlation coefficient of  $R = 0.71$  was found between the two results, a tropospheric NO<sub>2</sub> VCD of  $(1.41 \pm 0.27) \times 10^{16}$  molecules/cm<sup>2</sup> and an estimated associated flux of  $(3.45 \pm 0.89) \times 10^{-3}$  kg/s was measured close to the industrial area of Galati city on 13 August 2014, the only day that it was possible to determine the NO<sub>2</sub> flux.

Also, we showed that the stratospheric SCD derived from ground-based and airborne measurements correlates well with stratospheric NO<sub>2</sub> derived from observations by the OMI satellite sensor.

Based on this study, we conclude that the ULT is an efficient tool which allows determining with a high resolution the NO<sub>2</sub> distribution around urban or industrial sources. Also, the ULT-DOAS system is a very efficient tool for measuring fluxes due to its flexibility during the flights and the

possibility to access remote areas. The ULT-DOAS system might also constitute a promising tool for satellite validation and calibration under clear-sky conditions, especially for upcoming high-resolution sensors such as the TROPOMI/Sentinel-5 Precursor instrument to be launched in summer 2017.

**Acknowledgments:** The work of D.E. Constantin was supported by Project PN-II-RU-TE-2014-4-2584, a grant of the Romanian National Authority for Scientific Research and Innovation, CNCS-UEFISCDI. The DOMINO data product was taken from the ESA TEMIS archive ([www.temis.nl](http://www.temis.nl)) maintained at KNMI, The Netherlands.

**Author Contributions:** Daniel-Eduard Constantin and Alexis Merlaud conceived and designed the study; Daniel-Eduard Constantin analyzed the data; and Mirela Voiculescu, Carmelia Dragomir, Lucian Georgescu, Gaia Pinardi, Francois Hendrick and Michel Van Roozendael improved the paper.

**Conflicts of Interest:** The authors declare no conflict of interest.

## References

1. Solomon, S.; Portmann, R.W.; Sanders, R.W.; Daniel, J.S.; Madsen, W.; Bartram, B.; Dutton, E.G. On the role of nitrogen dioxide in the absorption of solar radiation. *J. Geophys. Res.* **1999**, *104*, 12047–12058. [[CrossRef](#)]
2. Platt, U. Differential optical absorption spectroscopy (DOAS). *Chem. Anal. Ser.* **1994**, *127*, 27–83.
3. Brewer, A.W.; McElroy, C.T.; Kerr, J.B. Nitrogen dioxide concentration in the atmosphere. *Nature* **1973**, *246*, 129–133. [[CrossRef](#)]
4. Noxon, J.F. Nitrogen dioxide in the stratosphere and troposphere measured by ground-based absorption spectroscopy. *Science* **1975**, *189*, 547–549. [[CrossRef](#)] [[PubMed](#)]
5. Hendrick, F.; Müller, J.-F.; Clémer, K.; Wang, P.; De Mazière, M.; Fayt, C.; Gielen, C.; Hermans, C.; Ma, J.Z.; Pinardi, G.; et al. Four years of ground-based MAX-DOAS observations of HONO and NO<sub>2</sub> in the Beijing area. *Atmos. Chem. Phys.* **2014**, *14*, 765–781. [[CrossRef](#)]
6. Constantin, D.-E.; Merlaud, A.; van Roozendael, M.; Voiculescu, M.; Fayt, C.; Hendrick, F.; Pinardi, G.; Georgescu, L. Measurements of Tropospheric NO<sub>2</sub> in Romania Using a Zenith-Sky Mobile DOAS System and Comparisons with Satellite Observations. *Sensors* **2013**, *13*, 3922–3940. [[CrossRef](#)]
7. Dragomir, C.; Constantin, D.-E.; Voiculescu, M.; Georgescu, L.; Merlaud, A.; Roozendael, M.V. Modeling results of atmospheric dispersion of NO<sub>2</sub> in an urban area using METI-LIS and comparison with coincident mobile DOAS measurements. *Atmos. Pollut. Res.* **2015**, *6*, 503–510. [[CrossRef](#)]
8. Merlaud, A.; van Roozendael, M.; van Gent, J.; Fayt, C.; Maes, J.; Toledo-Fuentes, X.; Ronveaux, O.; de Mazière, M. DOAS measurements of NO<sub>2</sub> from an ultralight aircraft during the Earth Challenge expedition. *Atmos. Meas. Tech.* **2012**, *5*, 2057–2068. [[CrossRef](#)]
9. Meier, A.C.; Schönhardt, A.; Bösch, T.; Richter, A.; Seyler, A.; Ruhtz, T.; Constantin, D.-E.; Shaiganfar, R.; Wagner, T.; Merlaud, A.; et al. High-resolution airborne imaging DOAS-measurements of NO<sub>2</sub> above Bucharest during AROMAT. *Atmos. Meas. Tech. Discuss.* **2016**. [[CrossRef](#)]
10. Tack, F.; Merlaud, A.; Iordache, M.-D.; Danckaert, T.; Yu, H.; Fayt, C.; Meuleman, K.; Deutsch, F.; Fierens, F.; van Roozendael, M. High resolution mapping of the NO<sub>2</sub> spatial distribution over Belgian urban areas based on airborne APEX remote sensing. *Atmos. Meas. Tech. Discuss.* **2017**. [[CrossRef](#)]
11. Merlaud, A.; Constantin, D.; Fayt, C.; Maes, J.; Mingireanu, F.; Mocanu, I.; Georgescu, L.; Roozendael, M. Small whiskbroom imager for atmospheric composition monitoring (SWING) from an unmanned areal vehicle (UAV). In Proceedings of the 21st ESA Symposium on European Rocket and Balloon Programmes and related Research, Thun, Switzerland, 9–13 June 2014; pp. 1–7.
12. Bovensmann, H.; Burrows, J.P.; Buchwitz, M.; Frerick, J.; Noël, S.; Rozanov, V.V.; Chance, K.V.; Goede, A.H.P. SCIAMACHY—Mission objectives and measurement modes. *J. Atmos. Sci.* **1999**, *56*, 127–150. [[CrossRef](#)]
13. Levelt, P.; van den Oord, G.; Dobber, M.; Malkki, A.; Visser, H.; de Vries, J.; Stammes, P.; Lundell, J.; Saari, H. The ozone monitoring instrument. *IEEE T. Geosci. Remote.* **2006**, *44*, 1093–1101. [[CrossRef](#)]
14. Munro, R.; Eisinger, M.; Anderson, C.; Callies, J.; Corpaccioli, E.; Lang, R.; Lefebvre, A.; Livschitz, Y.; Albinana, A.P. GOME-2 on MetOp. In Proceedings of the 2006 EUMETSAT Meteorological Satellite Conference, Helsinki, Finland, 12–16 June 2006; p. 48.
15. van der A, R.J.; Eskes, H.J.; Boersma, K.F.; van Noije, T.P.C.; van Roozendael, M.; de Smedt, I.; Peters, D.H.M.U.; Meijer, E.W. Trends, seasonal variability and dominant NO<sub>x</sub> source derived from a ten year record of NO<sub>2</sub> measured from space. *J. Geophys. Res.* **2008**, *113*, D04302. [[CrossRef](#)]

16. Varotsos, C.; Christodoulakis, J.; Tzanis, C.; Cracknell, A.P. Signature of tropospheric ozone and nitrogen dioxide from space: A case study for Athens, Greece. *Atmos. Environ.* **2014**, *89*, 721–730. [CrossRef]
17. Junkermann, W. An ultralight aircraft as platform for research in the lower troposphere: System performance and first results from radiation transfer studies in stratiform aerosol layers and broken cloud conditions. *J. Atmos. Ocean. Technol.* **2001**, *18*, 934. [CrossRef]
18. Junkermann, W. On the distribution of formaldehyde in the western Po-Valley, Italy, during FORMAT 2002/2003. *Atmos. Chem. Phys.* **2009**, *9*, 9187–9196. [CrossRef]
19. Chazette, P.; Sanak, J.; Dulac, F. New Approach for Aerosol Profiling with a Lidar Onboard an Ultralight Aircraft: Application to the African Monsoon Multidisciplinary Analysis. *Environ. Sci. Technol.* **2007**, *41*, 8335–8341. [CrossRef] [PubMed]
20. Wang, P.; Richter, A.; Bruns, M.; Burrows, J.P.; Scheele, R.; Junkermann, W.; Heue, K.-P.; Wagner, T.; Platt, U.; Pundt, I. Airborne multi-axis DOAS measurements of tropospheric SO<sub>2</sub> plumes in the Po-valley, Italy. *Atmos. Chem. Phys.* **2006**, *6*, 329–338. [CrossRef]
21. Grutter, M.; Basaldud, R.; Rivera, C.; Harig, R.; Junkerman, W.; Caetano, E.; Delgado-Granados, H. SO<sub>2</sub> emissions from Popocatepetl volcano: Emission rates and plume imaging using optical remote sensing techniques. *Atmos. Chem. Phys.* **2008**, *8*, 6655–6663. [CrossRef]
22. General, S.; Pöhler, D.; Sihler, H.; Bobrowski, N.; Frieß, U.; Zielcke, J.; Horbanski, M.; Shepson, P.B.; Stirm, B.H.; Simpson, W.R.; et al. The Heidelberg Airborne Imaging DOAS Instrument (HAIDI)—A novel imaging DOAS device for 2-D and 3-D imaging of trace gases and aerosols. *Atmos. Meas. Tech.* **2014**, *7*, 3459–3485. [CrossRef]
23. Liu, L.; Flatøy, F.; Ordóñez, C.; Braathen, G.O.; Hak, C.; Junkermann, W.; Andreani-Aksoyoglu, S.; Mellqvist, J.; Galle, B.; Prévôt, A.S.H.; et al. Photochemical modelling in the Po basin with focus on formaldehyde and ozone. *Atmos. Chem. Phys.* **2007**, *7*, 121–137. [CrossRef]
24. Airborne Romanian Measurements of Aerosols and Trace Gases (AROMAT). Available online: <http://uv-vis.aeronomie.be/aromat/index.php> (accessed on 15 January 2017).
25. Danckaert, T.; Fayt, C.; van Roozendaal, M.; de Smedt, I.; Letocart, V.; Merlaud, A.; Pinardi, G. QDOAS Software user manual Version 2.111–April 2016, UV-Visible DOAS Research Group of the Royal Belgian Institute for Space Aeronomy Web Site. Available online: [http://uv-vis.aeronomie.be/software/QDOAS/QDOAS\\_manual.pdf](http://uv-vis.aeronomie.be/software/QDOAS/QDOAS_manual.pdf) (accessed on 15 December 2016).
26. Vandaele, A.; Hermans, C.; Simon, P.; Carleer, M.; Colin, R.; Fally, S.; Mérienne, F.; Jenouvrier, A.; Coquart, B. Measurements of the NO<sub>2</sub> absorption cross-section from 42000 cm<sup>−1</sup> to 10000 cm<sup>−1</sup> (238–1000 nm) at 220 K and 294 K (220 K). *J. Quant. Spectrosc. Radiat. Transf.* **1998**, *59*, 171–184. [CrossRef]
27. Bogumil, K.; Orphal, J.; Homann, T.; Voigt, S.; Spietz, P.; Fleischmann, O.C.; Vogel, A.; Hartmann, M.; Kromminga, H.; Bovensmann, H.; et al. Measurements of molecular absorption spectra with the SCIAMACHY pre-flight model: Instrument characterization and reference data for atmospheric remote-sensing in the 230–2380 nm region. *J. Photochem. Photobiol. A Chem.* **2003**, *157*, 167–184. [CrossRef]
28. Thalman, R.; Volkamer, R. Temperature dependent absorption cross-sections of O<sub>2</sub>–O<sub>2</sub> collision pairs between 340 and 630 nm and at atmospherically relevant pressure. *Phys. Chem. Chem. Phys.* **2013**, *15*, 15371–15381. [CrossRef] [PubMed]
29. Chance, K.V.; Spurr, R.J.D. Ring effect studies: Rayleigh scattering, including molecular parameters for rotational Raman scattering, and the Fraunhofer spectrum. *Appl. Opt.* **1997**, *36*, 5224–5230. [CrossRef] [PubMed]
30. Baidar, S.; Oetjen, H.; Coburn, S.; Dix, B.; Ortega, I.; Sinreich, R.; Volkamer, R. The CU Airborne MAX-DOAS instrument: Vertical profiling of aerosol extinction and trace gases. *Atmos. Meas. Tech.* **2013**, *6*, 719–739. [CrossRef]
31. Vaughan, G.; Quinn, P.T.; Green, A.C.; Bean, J.; Roscoe, H.K.; van Roozendaal, M.; Goutail, F. SAOZ measurements of stratospheric NO<sub>2</sub> at Aberystwyth. *J. Environ. Monit.* **2006**, *8*, 353–361. [CrossRef] [PubMed]
32. Dirksen, R.J.; Boersma, K.F.; Eskes, H.J.; Ionov, D.V.; Bucsela, E.J.; Levelt, P.F.; Kelder, H.M. Evaluation of stratospheric NO<sub>2</sub> retrieved from the Ozone Monitoring Instrument: Intercomparison, diurnal cycle and trending. *J. Geophys. Res.* **2011**, *116*, D08305. [CrossRef]

33. Hendrick, F.; Barret, B.; van Roozendaal, M.; Boesch, H.; Butz, A.; De Mazière, M.; Goutail, F.; Hermans, C.; Lambert, J.-C.; Pfeilsticker, K.; et al. Retrieval of nitrogen dioxide stratospheric profiles from ground-based zenith-sky UV-visible observations: Validation of the technique through correlative comparisons. *Atmos. Chem. Phys.* **2004**, *4*, 2091–2106. [[CrossRef](#)]
34. Hendrick, F.; van Roozendaal, M.; Kylling, A.; Petritoli, A.; Rozanov, A.; Sanghavi, S.; Schofield, R.; von Friedeburg, C.; Wagner, T.; Wittrock, F.; et al. Intercomparison exercise between different radiative transfer models used for the interpretation of ground-based zenith-sky and multi-axis DOAS observations. *Atmos. Chem. Phys.* **2006**, *6*, 93–108. [[CrossRef](#)]
35. Mayer, B.; Kylling, A. Technical note: The libRadtran software package for radiative transfer calculations—Description and examples of use. *Atmos. Chem. Phys.* **2005**, *5*, 1855–1877. [[CrossRef](#)]
36. Rivera, C.; Sosa, G.; Wöhrnschimmel, H.; de Foy, B.; Johansson, M.; Galle, B. Tula industrial complex (Mexico) emissions of SO<sub>2</sub> and NO<sub>2</sub> during the MCMA 2006 field campaign using a mobile mini-DOAS system. *Atmos. Chem. Phys.* **2009**, *9*, 6351–6361. [[CrossRef](#)]
37. Johansson, M.; Rivera, C.; de Foy, B.; Lei, W.; Song, J.; Zhang, Y.; Galle, B.; Molina, L. Mobile mini-DOAS measurement of the outflow of NO<sub>2</sub> and HCHO from Mexico City. *Atmos. Chem. Phys.* **2009**, *9*, 5647–5653. [[CrossRef](#)]
38. Stein, A.F.; Draxler, R.R.; Rolph, G.D.; Stunder, B.J.B.; Cohen, M.D.; Ngan, F. NOAA's HYSPLIT atmospheric transport and dispersion modeling system. *Bull. Am. Meteorol. Soc.* **2015**, *96*, 2059–2077. [[CrossRef](#)]
39. *Studiu Privind Calitatea Aerului in Municipiul Galati*; Municipiul Galati: Galati, Romania, 2016.
40. Frins, E.; Bobrowski, N.; Osorio, M.; Casaballe, N.; Belsterli, G.; Wagner, T.; Platt, U. Scanning and mobile multi-axis DOAS measurements of SO<sub>2</sub> and NO<sub>2</sub> emissions from an electric power plant in Montevideo, Uruguay. *Atmos. Environ.* **2014**, *98*, 347–356. [[CrossRef](#)]



© 2017 by the authors. Licensee MDPI, Basel, Switzerland. This article is an open access article distributed under the terms and conditions of the Creative Commons Attribution (CC BY) license (<http://creativecommons.org/licenses/by/4.0/>).